nature immunology

Regulation of leukocyte recruitment by the long pentraxin PTX3

Livija Deban[1], Remo Castro Russo[1,2], Marina Sironi[1], Federica Moalli[1], Margherita Scanziani[4], Vanessa Zambelli[3,4], Ivan Cuccovillo[1], Antonio Bastone[3], Marco Gobbi[3], Sonia Valentino[1], Andrea Doni[1], Cecilia Garlanda[1], Silvio Danese[1], Giovanni Salvatori[5], Marica Sassano[6], Virgilio Evangelista[7], Barbara Rossi[8], Elena Zenaro[8], Gabriela Constantin[8], Carlo Laudanna[8], Barbara Bottazzi[1] & Alberto Mantovani[1,9]

Pentraxins are a superfamily of conserved proteins involved in the acute-phase response and innate immunity. Pentraxin 3 (PTX3), a prototypical member of the long pentraxin subfamily, is a key component of the humoral arm of innate immunity that is essential for resistance to certain pathogens. A regulatory role for pentraxins in inflammation has long been recognized, but the underlying mechanisms remain unclear. Here we report that PTX3 bound P-selectin and attenuated neutrophil recruitment at sites of inflammation. PTX3 released from activated leukocytes functioned locally to dampen neutrophil recruitment and regulate inflammation. Antibodies have glycosylation-dependent regulatory effect on inflammation. Therefore, PTX3, which is an essential component of humoral innate immunity, and immunoglobulins share functional outputs, including complement activation, opsonization and, as shown here, glycosylation-dependent regulation of inflammation.

Pentraxins constitute a superfamily of evolutionarily conserved proteins characterized by a cyclic multimeric structure[1]. *In vivo* functions for the classic short pentraxins C-reactive protein (CRP) and serum amyloid P component, produced mainly in the liver, have not been unequivocally defined because of considerable divergence between mouse and man in sequence and, most prominently, regulation (CRP is not an acute-phase protein in mice)[2]. PTX3 is the first member of the long pentraxin family. Unlike the classic short pentraxins, this molecule is highly conserved between mouse and man in terms of sequence, ligand recognition and regulation[3]. Macrophages, dendritic cells and endothelial cells are major producers of PTX3 in response to Toll-like receptor engagement[4] and inflammatory cytokines[5]. Neutrophil-specific granules serve as a source of ready-made PTX3 (ref. 6).

PTX3 has antibody-like functions, binding pathogens, activating and regulating complement and opsonizing particles[1,4,7–12]. In addition to having those recognition and effector functions, evidence exists showing that PTX3 can regulate inflammatory reactions[13–15], as also reported for the classic short pentraxins[16–19]. In particular, PTX3-transgenic mice show greater resistance than wild-type mice to lipopolysaccharide toxicity and to cecal ligation and puncture[13], whereas *Ptx3*$^{-/-}$ mice develop more myocardial damage associated with more neutrophil infiltration in a model of cardiac ischemia-reperfusion injury[15]. However, the molecular basis for the reported regulatory function of pentraxins in general and PTX3 in particular in inflammatory reactions remains largely undefined.

The cell-migration process that causes leukocyte emigration to extravascular sites is essential to the innate and adaptive immune responses[20]. Leukocyte recruitment in acute and chronic inflammation entails a cascade of sequential cell-adhesion and cell-activation events, including tethering, rolling, adhesion, diapedesis, transmigration and chemotaxis[21,22]. The selectin family of cell-adhesion molecules consists of three calcium-dependent lectins: L-selectin (CD62L; A001417), which is constitutively expressed on most leukocytes; E-selectin (CD62E), which is expressed exclusively on endothelial cells after cytokine stimulation; and P-selectin (CD62P), which is stored on membranes of endothelial Weibel-Palade bodies and platelet α-granules[20]. Selectins interact with cell-surface glycoconjugates[23] and mediate leukocyte tethering and rolling, thereby bringing circulating leukocytes into proximity with extracellular stimuli such as cytokines, chemokines and chemoattractants that are displayed on or released from activated endothelium[24]. After cells encounter inflammatory and thrombogenic stimuli, P-selectin rapidly relocates to the cell surface and binds P-selectin glycoprotein 1 (PSGL-1) expressed on leukocytes. This interaction mediates the tethering and rolling of both leukocytes and platelets on activated endothelial cells, as well as heterotypic aggregation between activated platelets and leukocytes[25]. Extensive studies of mice lacking selectins have elucidated

[1]Laboratory for Immunology and Inflammation, Instituto di Ricovero e Cura a Carattere Scientifico–Istituto Clinico Humanitas, Rozzano, Italy. [2]Laboratório de Imunofarmacologia, Departamento de Bioquímica e Imunologia, Instituto de Ciências Biológicas, Universidade Federal de Minas Gerais, Belo Horizonte, Minas Gerais, Brazil. [3]Mario Negri Institute, Milan, Italy. [4]Department of Experimental Medicine, University of Milano-Bicocca, Milan, Italy. [5]Sigma-Tau Research and Development, Pomezia, Italy. [6]Tecnogen, Ricerca e Sviluppo, Piana di Monte Verna, Italy. [7]Consorzio Mario Negri Sud, Santa Maria Imbaro, Italy. [8]Department of Pathology, University of Verona, Verona, Italy. [9]Dipartimento di Medicina Traslazionale, University of Milan, Milan, Italy. Correspondence should be addressed to A.M. (alberto.mantovani@humanitasresearch.it).

Received 11 January; accepted 12 February; published online 7 March 2010; doi:10.1038/ni.1854

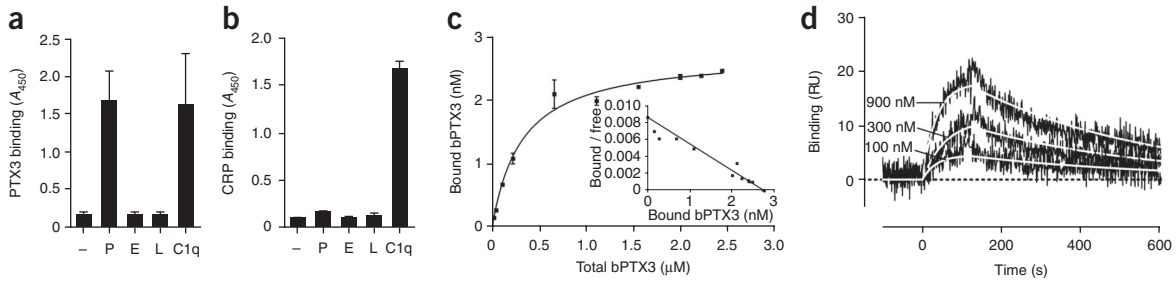

Figure 1 Interaction of PTX3 with P-selectin. (**a**,**b**) Microtiter plate assay of the binding of PTX3 (220 nM; **a**) or CRP (470 nM; **b**) to plates coated with P-selectin (P), E-selectin (E) or L-selectin (L), presented as absorbance at 450 nm (A_{450}). C1q serves as a positive control. Results are from three independent experiments (mean and s.d. of duplicate or triplicate wells). (**c**) Affinity of the interaction between P-selectin immobilized on microtiter wells and various amounts of biotinylated PTX3 (bPTX3); specific binding was measured in accordance with a standard curve of bPTX3, with nonlinear fitting analysis. Inset, Scatchard plot of binding data. Data are representative of four experiments (error bars, s.d.). (**d**) SPR analysis of the binding of 100, 300 and 900 nM P-selectin injected onto immobilized PTX3. Sensorgrams were fitted by the 1:1 interaction model (white lines) to obtain the corresponding association and dissociation rate constants (k_{on} and k_{off}) and are presented as time course of the SPR signal in resonance units (RU). Data are representative of two experiments.

a central role for P-selectin in leukocyte and platelet rolling and early leukocyte recruitment into inflammatory sites[26–28].

In the context of a comprehensive effort to determine the PTX3 interactome[29], we sought to elucidate the mechanisms underlying the role of PTX3 in inflammation. Our focus was on the initial event of the inflammatory process: the rolling of leukocytes on inflamed blood vessels. We identified a selective, glycosylation-dependent interaction of PTX3 with P-selectin that dampened neutrophil recruitment at sites of inflammation.

RESULTS

PTX3 binds P-selectin

To determine whether PTX3 can interact with key molecules involved in leukocyte rolling, we assayed selectins for PTX3 binding. The short pentraxin serum amyloid P component has been shown to bind selectins, although the functional relevance of this interaction has not been determined[30]. In a microtiter plate assay, recombinant human PTX3 selectively bound recombinant human P-selectin and not E- or L-selectin (**Fig. 1a**). We examined the interaction of the short pentraxin CRP with selectins and found that CRP did not bind selectins in our experimental setting (**Fig. 1b**). We calculated an apparent dissociation constant (K_d) of 360 ± 30 nM (mean of four experiments) for the binding of recombinant PTX3 to immobilized P-selectin when we added serial dilutions of biotinylated PTX3 to P-selectin-coated wells and evaluated the amount of bound PTX3 on the basis of a standard curve of the biotinylated protein (**Fig. 1c**).

We further characterized the binding of recombinant PTX3 to P-selectin by surface plasmon resonance (SPR). SPR studies showed that unlike the very fast association and dissociation rates that characterize the interaction of P-selectin with its classic ligand PSGL-1 (refs. 31,32), the binding of P-selectin to PTX3 was characterized by lower association (k_{on}) and dissociation (k_{off}) rate constants (k_{on}, $2.3 \times 10^4 \pm 0.7 \times 10^4\ M^{-1}s^{-1}$, and k_{off}, $2.9 \times 10^{-3} \pm 1.5 \times 10^{-3}\ s^{-1}$) with a K_d of 123 nM (**Fig. 1d**). Human PTX3 purified from freshly isolated human neutrophils bound P-selectin (**Fig. 2a**) but not E-selectin or L-selectin (**Supplementary Fig. 1**). We estimated neutrophil-derived PTX3 to be at least ten times more potent in binding P-selectin than was recombinant PTX3 expressed by eukaryotic (Chinese hamster ovary (CHO)) cells in a series of four experiments. This difference was probably a reflection of heterogeneity that might have been due to differences in PTX3 glycosylation. Heterogeneity in the relative amount of bi-, tri- and tetra-antennary glycosylated structures, as well as that of variably sialylated oligosaccharides, has been observed among the different sources of PTX3 (ref. 33 and unpublished data). In severe inflammatory conditions, PTX3 is present in the circulation at submicromolar concentrations[34,35]. Therefore, the affinity of PTX3 for P-selectin is compatible with its being relevant *in vivo*. Natural polymorphonuclear neutrophil (PMN)-derived PTX3 was more potent than recombinant PTX3, and higher effective concentrations could be reached locally in the microcirculation. We therefore further characterized the PTX3–P-selectin interaction *in vitro* and its relevance *in vivo*.

Mapping of the interaction site on PTX3

The mature PTX3 protein is composed of two domains encoded by different exons. In a PTX3 monomer, a unique N-terminal domain, encoded by the second exon, is coupled to the pentraxin (C-terminal) domain, encoded by the third exon. Monomers can associate into octamers stabilized by disulfide bridges[36]. To better understand this interaction, we investigated which PTX3 domain is involved in the interaction with P-selectin. The recombinant C-terminal domain bound to P-selectin, whereas the N-terminal domain showed no binding (**Fig. 2a**). We confirmed the binding of the recombinant C-terminal domain of PTX3 to P-selectin by SPR (**Fig. 2b**).

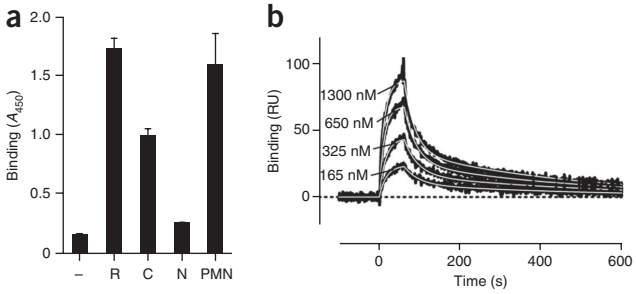

Figure 2 Binding site for P-selectin on PTX3. (**a**) Microtiter plate assay of the binding of recombinant PTX3 (R; 220 nM), its recombinant C- and N-terminal domains (C (220 nM) and N (220 nM), respectively) and PMN-derived PTX3 (PMN; 5 nM) to P-selectin. Results are from three independent experiments (mean and s.d. of duplicate or triplicate wells). (**b**) SPR analysis of the binding of 165, 325, 650 and 1300 nM P-selectin injected onto the immobilized C-terminal domain of PTX3, presented as the time course of the SPR signal. Sensorgrams were fitted by a model that included two different K_d values (white lines). Data are representative of two experiments.

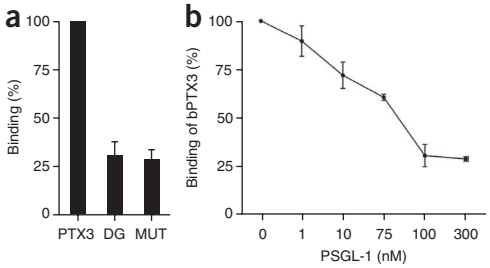

Figure 3 The role of the PTX3 glycosidic moiety in the PTX3–P-selectin interaction. (**a**) Binding of untreated PTX3 (PTX3; 220 nM), enzymatically deglycosylated PTX3 (DG; 220 nM) or PTX3 deglycosylated by site-directed mutagenesis (MUT; 220 nM) to P-selectin-coated wells. Results are from four independent experiments (mean and s.d. of duplicate wells). (**b**) Binding of PTX3 (110 nM) to P-selectin-coated wells in the presence of increasing doses of recombinant PSGL-1, presented as percentage of binding in the absence of PSGL-1. Results are from four independent experiments (mean ± s.d. of duplicate wells).

Sensorgrams could not be adequately fitted by the 1:1 interaction model and required a more complex equation. A model that included two different K_d values (probably due to some conformational heterogeneity of the immobilized protein) resulted in good fitting of experimental data; the K_d values obtained by analysis of 11 sensorgrams (with P-selectin concentrations ranging from 100 to 1,300 nM) were as follows: 78 nM (k_{on}, $2.9 \pm 0.8 \times 10^4$ $M^{-1}s^{-1}$; k_{off}, $2.2 \pm 0.7 \times 10^{-3}$ s^{-1}) and 430 nM (k_{on}, $10.2 \pm 7 \times 10^4$ $M^{-1}s^{-1}$; k_{off}, $3.2 \pm 0.9 \times 10^{-2}$ s^{-1}). Thus, the PTX3–P-selectin interaction is mediated by the pentraxin domain of PTX3.

The importance of the glycosidic moiety

The C-terminal domain of PTX3 contains a single N-glycosylation site on Asn220 linked to fucosylated and sialylated biantennary complex–type sugars[33]. Because selectins bind to carbohydrate moieties that are present on certain carrier molecules[37], we tested the involvement of the PTX3 glycosidic moiety. Both enzymatic deglycosylation of PTX3 and site-directed mutagenesis of its glycosylation-carrying residue (Asn220 to Gln220) resulted in binding to P-selectin that was 70% lower (**Fig. 3a**). Deglycosylated PTX3 remained functional in other assays: it bound C1q (the first component of the classical complement cascade), the extracellular matrix protein TSG6 and microbial moieties at least as efficiently as the native molecule did[33] (**Supplementary Fig. 2**). We next assessed whether PSGL-1 can compete with PTX3 for binding to P-selectin. Indeed, the addition of PSGL-1 to the assay diminished the binding of PTX3 to P-selectin in a dose-dependent manner (**Fig. 3b** and **Supplementary Fig. 3**). PTX3 did not bind PSGL-1 in the same experimental conditions (**Supplementary Fig. 4**). In the *in vitro* system used, consisting of a PSGL-1 fusion protein and polyclonal antibodies, recombinant PTX3 failed to efficiently displace binding to P-selectin, most probably because of the lower k_{on} value, as discussed above (data not shown). This finding may indicate that PTX3 derived from arrested PMNs will not interfere in an autocrine way with the adhesive and signaling functions of PSGL-1. Together these data suggest that PTX3 acts as a competitive inhibitor of the P-selectin–PSGL-1 interaction.

The PTX3–P-selectin interaction in a cell-based context

Having characterized the biochemical properties of the PTX3–P-selectin interaction, we next assessed whether PTX3 bound P-selectin in a more physiological context. PTX3 bound in a dose-dependent manner to P-selectin-transfected CHO cells (**Fig. 4a**), whereas we observed no binding to untransfected or irrelevant protein–transfected CHO cells (**Supplementary Fig. 5**). Furthermore, thrombin-activated platelets expressing P-selectin bound PTX3, and this binding was inhibited by function-blocking antibody to P-selectin (anti-P-selectin; **Fig. 4b**), which suggested a physiological relevance for this interaction.

P-selectin is stored in Weibel-Palade bodies of endothelial cells, and after activation, it relocates rapidly to the cell surface, where it has an essential role in the early stages (tethering and rolling) of leukocyte recruitment[38]. Together the data presented above suggested that PTX3 might compete with leukocyte PSGL-1 for P-selectin binding during the initial steps of the leukocyte extravasation cascade. We addressed

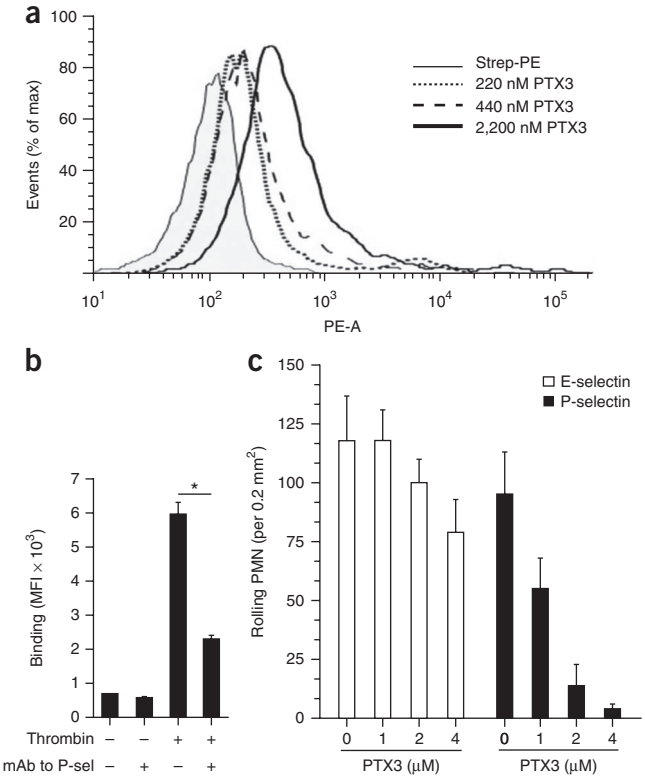

Figure 4 PTX3 binds P-selectin in a cell-based context. (**a**) Binding of PTX3 to P-selectin-transfected CHO cells, assessed by flow cytometry. Results are presented as the percentage of maximum (% of max) to allow the presentation of normalized data and represent the number of events in each bin divided by the number of events in the bin with the largest number of cells. PE-A (horizontal axis), area under the curve for the intensity of phycoerythrin fluorescence. Mean fluorescence intensity (MFI): streptavidin-phycoerythrin (Strep-PE), 119.62; 220 nM PTX3, 996.02; 440 nM PTX3, 2309.71; 2,200 nM PTX3, 5768.92. Data are representative of two independent experiments. (**b**) Binding of PTX3 (1 μM) to resting or thrombin-activated platelets in the presence or absence of a monoclonal P-selectin-blocking antibody (mAb to P-sel (CLB-Thromb/6); 20 μg/ml), assessed by flow cytometry. $^*P < 0.001$ (one-way analysis of variance (ANOVA)). Data are representative of three experiments (mean and s.d.). (**c**) Analysis of leukocyte rolling on P-selectin- and E-selectin-coated glass capillary tubes in the presence of increasing doses of PTX3; results were recorded for single areas of 0.2 mm^2 for at least 30 s. Rolling interactions (corresponding to interactions lasting less than 0.5 s) were considered important and were given scores. Data are from five experiments with five to seven areas analyzed in each (mean and s.d.).

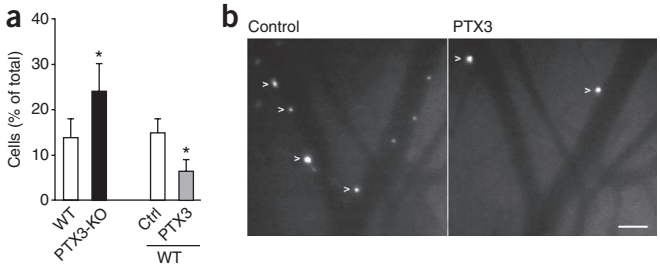

Figure 5 PTX3 inhibits rolling interactions *in vivo*. (**a**) Frequency of rolling interactions of PMNs in the mesenteric venules of wild-type mice (WT) and *Ptx3*$^{-/-}$ mice (PTX3-KO) and in wild-type mice with (PTX3) or without (Ctrl) PTX3 pretreatment (right), presented as rolling fractions (venules and mice per group, **Supplementary Tables 1** and **2**). *$P < 0.01$ (paired or unpaired two-tailed Student's *t*-test). Data are representative of five experiments (mean and s.e.m.). (**b**) Rolling PMNs (arrowheads) after thrombin stimulation in mesenteric venules before PTX3 administration (Control) and after PTX3 treatment (PTX3). Scale bar, 50 μm. Data are representative of five experiments.

this hypothesis in an *in vitro* rolling assay. The rolling of freshly isolated human neutrophils on P-selectin-coated glass capillaries under a shear stress of 2 dyne/cm^2 was strongly inhibited by pretreatment of the coated capillaries with PTX3 (**Fig. 4c**). PTX3 pretreatment had little effect on E-selectin-mediated rolling *in vitro*. PTX3 itself did not support the rolling of neutrophils or monocytes under shear stress when it was coated onto glass capillaries (data not shown). Thus, PTX3 blocks the rolling of leukocytes on P-selectin in an *in vitro* setting.

In vivo analysis of leukocyte rolling

Next we addressed the role of PTX3 in leukocyte rolling *in vivo*. We made a comparative analysis of rolling by intravital microscopy of thrombin-stimulated mesenteric venules. This analysis showed that *Ptx3*$^{-/-}$ mice had significantly (71%) more rolling interactions than did wild-type mice (**Fig. 5a** and **Supplementary Table 1**). Moreover, the administration of PTX3 to wild-type mice consistently attenuated the frequency of rolling interactions (55% inhibition; **Fig. 5** and **Supplementary Table 2**). The strength and quality of rolling interactions (frequency distributions of rolling velocities) were not influenced much by genetic deficiency or PTX3 administration (**Supplementary Fig. 6** and **Supplementary Tables 1** and **2**). These data show that endogenously secreted PTX3 can indeed affect leukocyte rolling *in vivo* and suggest that PTX3 can attenuate extravasation under pathological conditions.

Exogenous PTX3 blocks PMN recruitment *in vivo*

The results discussed above suggested that PTX3 may exert an anti-inflammatory effect in P-selectin-dependent models of leukocyte recruitment and inflammation. The recruitment of neutrophils into the pleural cavity during the early stages of pleural inflammation in response to the CXC chemokine KC (CXCL1; A003780) is dependent on P-selectin and L-selectin[39], and we adapted this model to test the *in vivo* functional consequences of the PTX3–P-selectin interaction[40]. Treatment with PTX3 resulted in 73% less accumulation of neutrophils measured at 2 h after injection of KC into the pleural cavity (**Fig. 6a**). The effect was dose dependent (**Supplementary Fig. 7a**). Exogenously administered PTX3 was rapidly cleared from the circulation with a half-life of 1 h (**Supplementary Fig. 8**). PTX3 administered 1 h after KC injection had no substantial activity. As expected on the basis of high sequence similarity between the human and mouse proteins[1], mouse PTX3 was also an effective inhibitor of leukocyte recruitment in this model (**Supplementary Fig. 9**). The inhibitory effect of PTX3 was similar to that of the P-selectin-blocking antibody (**Fig. 6a**). Heat inactivation of PTX3 before administration abrogated the inhibitory effect of the intact molecule (**Fig. 6a**). In addition, lack of PTX3 glycosylation due to site-directed mutagenesis of Asn220 also reversed the inhibitory effect of the wild-type molecule, an observation consistent with *in vitro* data on the involvement of the sugar moiety (**Fig. 6a**). Notably, treatment with the C-terminal domain of recombinant PTX3 impaired early neutrophil recruitment similarly to the full-length protein (**Fig. 6a**), which suggested that the C terminus is sufficient for this anti-inflammatory effect of PTX3. We did not observe the inhibitory effect of PTX3 on recruitment in the presence of P-selectin-blocking antibody or in P-selectin-deficient mice (**Fig. 6b**). In addition, the inhibitory effect of PTX3 was reproduced when we used lipopolysaccharide as the inflammatory stimulus instead of KC (**Fig. 6c**). Time-course experiments showed that treatment with PTX3 caused an overall lower PMN accumulation in the pleurisy model over 18 h, by which time neutrophil numbers returned to baseline (**Supplementary Fig. 7b**). These data suggest that PTX3 attenuates, rather than simply delaying, the accumulation of neutrophils at sites of inflammation. Using bone marrow chimeras, we found that P-selectin-deficient mice reconstituted with either P-selectin-deficient or wild-type bone marrow showed impairment of PMN recruitment (data not shown), which suggested that platelets do not have a role in the pleurisy model. Further work with the appropriate models (such as experimental atherosclerosis) is needed to investigate the importance of the recognition of platelet P-selectin by PTX3.

Hematopoietic cell–derived PTX3 dampens PMN extravasation

PTX3 is stored in neutrophil-specific granules and is released after PMN degranulation[6], and it is also produced by diverse cell

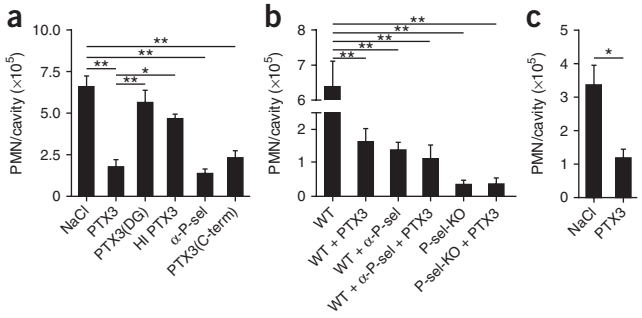

Figure 6 Exogenous PTX3 dampens early leukocyte recruitment *in vivo*. (**a**) Recruitment of PMNs into the pleural cavity of wild-type mice treated intravenously with vehicle (0.9% saline solution (NaCl); $n = 15$), PTX3 (100 μg/mouse; $n = 15$), deglycosylated PTX3 (PTX3(DG); 100 μg/mouse; $n = 8$), heat-inactivated PTX3 (HI PTX3; 100 μg/mouse; $n = 6$), P-selectin-blocking antibody (α-P-sel; 30 μg/mouse; $n = 8$) or the C-terminal domain of PTX3 (PTX3(C-term); 100 μg/mouse; $n = 8$) 10 min before intrapleural injection of KC. (**b**) Recruitment of PMNs into the pleural cavity of wild-type and P-selectin-deficient (P-sel-KO) mice pretreated intravenously with vehicle (0.9% saline solution; wild type, $n = 14$; P-selectin-deficient, $n = 8$), PTX3 (100 μg/mouse; wild type, $n = 15$; P-selectin-deficient, $n = 7$), P-selectin-blocking antibody (30 μg/mouse; $n = 15$) or PTX3 and the P-selectin-blocking antibody together ($n = 8$). (**c**) Recruitment of PMNs into the pleural cavity of wild-type mice pretreated intravenously with vehicle (0.9% saline solution; $n = 15$) or PTX3 (100 μg/mouse; $n = 15$), assessed 2 h after injection of lipopolysaccharide (400 ng/mouse). *$P < 0.01$ and **$P < 0.001$ (one-way ANOVA). Data are representative two to six different experiments (**a**,**b**) or two experiments (**c**; mean and s.e.m.).

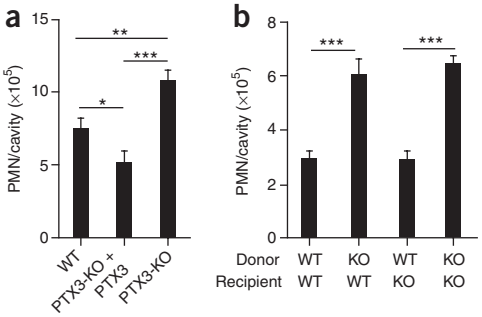

Figure 7 Role of endogenous PTX3 in leukocyte recruitment. (**a**) Recruitment of PMNs into the pleural cavity of wild-type and PTX3-deficient mice pretreated intravenously with vehicle (0.9% saline solution; wild type, $n = 16$; PTX3-deficient, $n = 16$) or PTX3 (PTX3-KO + PTX3; 100 μg/mouse; $n = 13$). (**b**) Recruitment of PMNs into the pleural cavity of lethally irradiated wild-type (WT) and PTX3-deficient (KO) mice that received wild-type or PTX3-deficient bone marrow (wild type→wild type, $n = 13$; PTX3-deficient→wild type, $n = 20$; wild type→PTX3-deficient, $n = 12$; PTX3-deficient→PTX3-deficient, $n = 11$). $^*P < 0.05$, $^{**}P < 0.01$ and $^{***}P < 0.001$ (one-way ANOVA). Data are representative of two experiments (**a**) or one experiment (**b**; mean and s.e.m.).

types, including endothelial cells, after inflammatory stimuli[5,41,42]. To evaluate the effect of endogenous PTX3 on leukocyte recruitment, we assessed the magnitude of neutrophil influx in *Ptx3*$^{-/-}$ mice in the pleural inflammation model. *Ptx3*$^{-/-}$ mice showed significantly more neutrophil accumulation than did wild-type mice (**Fig. 7a**). This phenotype was reversed by treatment with exogenous PTX3 (**Fig. 7a**). In an effort to delineate the relative contributions of hematopoietic cell–derived PTX3 and stromal cell–derived PTX3, we used bone marrow chimeras. Wild-type mice that received *Ptx3*$^{-/-}$ bone marrow showed more neutrophil influx than did mice transplanted with wild-type bone marrow, a phenotype resembling that of *Ptx3*$^{-/-}$ mice (**Fig. 7b**). Conversely, in *Ptx3*$^{-/-}$ mice that received wild-type bone marrow, the number of recruited cells was similar to that of wild-type mice (**Fig. 7b**). The localization of PTX3 in neutrophil granules is selective in that eosinophils, basophils, platelets, natural killer cells and endothelial cells are negative for this[6]. Moreover, chemokines do not induce gene expression–dependent production of PTX3 in monocytes and dendritic cells[3]. Therefore, these results suggest that in the pleurisy model, at least at early time points, neutrophils are the main source of PTX3, which acts as a negative feedback loop for PMN recruitment.

PTX3 dampens PMN recruitment in acute lung injury

P-selectin has long been known to be involved in some models of inflammatory recruitment of neutrophils into the lung[43]. Acute lung injury, which leads to acute respiratory distress syndrome, is a common disease with an incidence of 79 per 100,000 person-years in the United States[44]. Despite the use of state-of-the-art treatment, this disease is associated with high mortality (up to 38%). Pneumonia and acid aspiration are typical causes of intrapulmonary acute lung injury. The recruitment of PMNs into the lungs is a key event in the development of this disorder[45]. Studies suggest that P-selectin-mediated platelet-neutrophil interactions are a chief contributor to acid-induced recruitment of PMNs and lung damage. In a mouse model of acid-induced acute lung injury (a model of acute respiratory distress syndrome), it has been demonstrated that blocking of P-selectin decreases the development of experimental early acid-induced acute lung injury[46]. We investigated whether PTX3 could also block P-selectin-mediated neutrophil extravasation in this animal model. Indeed, treatment with PTX3 before the induction of lung damage resulted in less accumulation of neutrophils in the lung (**Fig. 8a**), as well as less migration of neutrophils into the bronchoalveolar space (**Fig. 8b**), similarly to treatment with anti-P-selectin. *Ptx3*$^{-/-}$ mice showed greater susceptibility to acid-induced lung injury in terms of wasting and lung function (in one experiment; **Supplementary Fig. 10**). For example, on day 2, loss of body weight was 4% ± 0.6% (mean ± s.e.m.) and 12% ± 1% in wild-type mice ($n = 9$) and *Ptx3*$^{-/-}$ mice ($n = 17$), respectively, and this effect was reversed by exogenous PTX3. Similarly, lung compliance was 1.52 ± 0.07 (mean ± s.e.m.) for wild-type mice ($n = 12$) and 1.70 ± 0.03 for PTX3-treated mice ($n = 12$; $P = 0.03$). Together these results suggest that PTX3 released from cells of bone marrow origin, most probably neutrophils, acts as a negative feedback mechanism that dampens P-selectin-dependent recruitment of leukocytes.

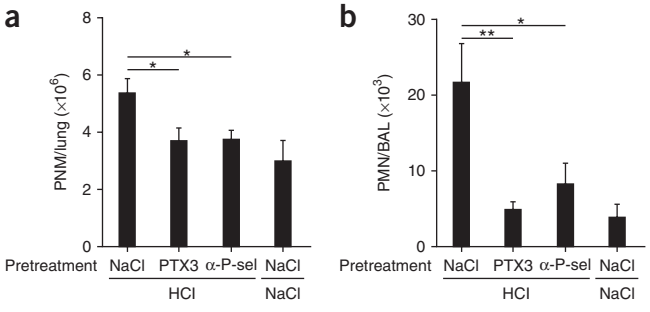

Figure 8 PTX3 dampens PMN recruitment in a model of acid-induced acute lung injury. (**a**) PMN infiltration of lung interstitium at 3 h after acid-induced acute lung injury (HCl) in mice pretreated intravenously with vehicle (0.9% saline solution; $n = 13$), PTX3 (100 μg/mouse; $n = 16$) or P-selectin-blocking antibody (30 μg/mouse; $n = 6$). (**b**) Migration of neutrophils into the bronchoalveolar space at 3 h after acid-induced acute lung injury in mice pretreated intravenously with vehicle (0.9% saline solution; $n = 7$), PTX3 (100 μg/mouse; $n = 8$) or P-selectin-blocking antibody (30 μg/mouse; $n = 6$). $^*P < 0.05$ and $^{**}P < 0.01$ (one-way ANOVA). Data are representative of two experiments (mean and s.e.m.).

DISCUSSION

Leukocyte infiltration can function as a double-edged sword, causing not only the mobilization of defense and tissue-repairing elements but also further tissue damage, as observed in ischemia-reperfusion injury, shock, systemic septicemia, transplantation and acute lung injury. Our results presented here have shown that the long pentraxin PTX3 selectively bound P-selectin via its N-linked glycosidic moiety located in the third exon–encoded pentraxin domain. Using three *in vivo* models of P-selectin-dependent inflammation (pleurisy, acid-induced acute respiratory distress syndrome and intravital microscopy analysis of mesenteric inflammation), we found that exogenous PTX3 and endogenous PTX3 released from hematopoietic cells acted as a negative feedback loop, preventing excessive P-selectin-dependent recruitment of neutrophils. Our results suggest that under conditions of massive leukocyte activation, the release of PTX3 acts locally as a negative feedback mediator, dampening neutrophil recruitment. It is likely that this pathway underlies the long-known regulatory role of PTX3 in inflammation. Our findings may affect the optimization and exploitation of the antimicrobial activity of pentraxins.

Our study here and published studies have suggested that the fluid-phase pattern-recognition molecule PTX3 can act as double-edged sword. After binding to microbial moieties[4,10–12], it has opsonic activity, activates complement and enhances leukocyte

recruitment[7]. However, as shown here, PTX3 can act as a regulatory molecule of innate immunity and inflammation by dampening excessive neutrophil recruitment. The results presented here suggest two scenarios in which PTX3 can exert a regulatory effect on inflammatory reactions. In localized inflammatory reactions, degranulation of neutrophils results in local PTX3 in the microcirculation, which, by binding P-selectin with a low dissociation rate (k_{off}, 2.9×10^{-3} s^{-1}), dampens excessive recruitment. In contrast, under conditions of systemic inflammation, such as sepsis and acute respiratory distress syndrome, high concentrations of circulating PTX3, reflecting release from degranulating neutrophils as well as gene expression–dependent production, can act systemically as a negative feedback loop.

PTX3 is a component of the humoral arm of the innate immune system that is conserved in evolution and is endowed with an essential role in resistance to certain pathogens, such as *Aspergillus fumigatus* and influenza virus[11,47]. It binds microbial moieties[4], orchestrates complement activation[8,9] and has opsonic activity[10]. Therefore, it acts as a functional predecessor of antibodies (an 'ante-antibody'). The finding of a regulatory function mediated by the glycosidic moiety is reminiscent of a similar activity of immunoglobulins[48]. Thus, immunoglobulins and components of the humoral arm of the innate immune system, such as pentraxins, although they are genetically and structurally different, share fundamental functional outputs, including agglutination, complement activation, opsonization and, as reported here, glycosylation-dependent regulation of inflammation.

METHODS

Methods and any associated references are available in the online version of the paper at http://www.nature.com/natureimmunology/.

Accession codes. UCSD-Nature Signaling Gateway (http://www.signaling-gateway.org): A001417 and A003780.

Note: Supplementary information is available on the Nature Immunology website.

ACKNOWLEDGMENTS

We thank D. Vestweber (Max Planck Institute for Molecular Biomedicine) for blocking monoclonal antibody to mouse P-selectin (Rb40.34); M. Locati (Istituto Clinico Humanitas, Rozzano, and University of Milan) for CHO cells transfected with the chemokine decoy receptor D6; G. Kansas (Northwestern University) for P-selectin-transfected CHO cells. F. Fumagalli (Istituto di Ricerche Farmacologiche Mario Negri) and M. Amigoni (University of Milano-Bicocca) for support in acute lung injury experiments; M. Stravalaci for assistance; and members of the Laboratory for Immunology and Inflammation for advice and discussions. Supported by the European Commission (HEALTH-F4-2008-202156 TOLERAGE), the European Research Council (project HIIS), Telethon (GGP05095), the Cassa di Risparmio delle Provincie Lombarde Foundation (NOBEL project), Ministero Università e Ricerca (MIUR–FIRBRBLA039LSF), the University of Milan (FIRST project), the Fondazione Humanitas per la Ricerca and Italian Association for Cancer Research, the International Graduate School in Molecular Medicine (Vita-Salute San Raffaele University, Italy; L.D.), the European Molecular Biology Organization (ASTF 293-2008 to L.D.), the National Institutes of Health (HL080166 to V.E.), the Fondazione Cariverona, Italian Ministry of Education and Research (G.C.), Fondazione Italiana Sclerosi Multipla, Genova, Italy (G.C.) and the National Multiple Sclerosis Society (G.C.).

AUTHOR CONTRIBUTIONS

L.D., B.B. and A.M. planned the research, analyzed and interpreted data and wrote the manuscript; L.D., R.C.R., M.Sironi., F.M., M.Scanziani and V.Z. did the animal experiments; A.B. and M.G. did the SPR experiments; C.L. did and analyzed leukocyte rolling experiments; S.V. and I.C. participated in purification of recombinant proteins and helped with mouse breeding and genotyping; L.D. and A.D. did and analyzed flow cytometry and microtiter plate binding assays; G.S. generated deglycosylated PTX3 by enzymatic digestion; M.Sassano. generated deglycosylated PTX3 by site-directed mutagenesis; G.C., B.R. and E.Z. did and analyzed the intravital microscopy experiments; and C.G., V.E. and S.D. contributed to data analysis and interpretation.

COMPETING FINANCIAL INTERESTS

The authors declare competing financial interests: details accompany the full-text HTML version of the paper at http://www.nature.com/natureimmunology/.

Published online at http://www.nature.com/natureimmunology/.
Reprints and permissions information is available online at http://npg.nature.com/reprintsandpermissions/.

1. Garlanda, C., Bottazzi, B., Bastone, A. & Mantovani, A. Pentraxins at the crossroads between innate immunity, inflammation, matrix deposition, and female fertility. *Annu. Rev. Immunol.* **23**, 337–366 (2005).
2. Pepys, M.B. & Hirschfield, G.M. C-reactive protein: a critical update. *J. Clin. Invest.* **111**, 1805–1812 (2003).
3. Bottazzi, B. *et al.* The long pentraxin PTX3 as a prototypic humoral pattern recognition receptor: interplay with cellular innate immunity. *Immunol. Rev.* **227**, 9–18 (2009).
4. Jeannin, P. *et al.* Complexity and complementarity of outer membrane protein A recognition by cellular and humoral innate immunity receptors. *Immunity* **22**, 551–560 (2005).
5. Doni, A. *et al.* Regulation of PTX3, a key component of humoral innate immunity in human dendritic cells: stimulation by IL-10 and inhibition by IFN-γ. *J. Leukoc. Biol.* **79**, 797–802 (2006).
6. Jaillon, S. *et al.* The humoral pattern recognition receptor PTX3 is stored in neutrophil granules and localizes in extracellular traps. *J. Exp. Med.* **204**, 793–804 (2007).
7. Cotena, A. *et al.* Complement dependent amplification of the innate response to a cognate microbial ligand by the long pentraxin PTX3. *J. Immunol.* **179**, 6311–6317 (2007).
8. Nauta, A.J. *et al.* Biochemical and functional characterization of the interaction between pentraxin 3 and C1q. *Eur. J. Immunol.* **33**, 465–473 (2003).
9. Deban, L. *et al.* Binding of the long pentraxin PTX3 to factor H: interacting domains and function in the regulation of complement activation. *J. Immunol.* **181**, 8433–8440 (2008).
10. Diniz, S.N. *et al.* PTX3 function as an opsonin for the dectin-1-dependent internalization of zymosan by macrophages. *J. Leukoc. Biol.* **75**, 649–656 (2004).
11. Garlanda, C. *et al.* Non-redundant role of the long pentraxin PTX3 in anti-fungal innate immune response. *Nature* **420**, 182–186 (2002).
12. Soares, A.C. *et al.* Dual function of the long pentraxin PTX3 in resistance against pulmonary infection with *Klebsiella pneumoniae* in transgenic mice. *Microbes Infect.* **8**, 1321–1329 (2006).
13. Dias, A.A. *et al.* TSG-14 transgenic mice have improved survival to endotoxemia and to CLP-induced sepsis. *J. Leukoc. Biol.* **69**, 928–936 (2001).
14. Ravizza, T. *et al.* Dynamic induction of the long pentraxin PTX3 in the CNS after limbic seizures: evidence for a protective role in seizure-induced neurodegeneration. *Neuroscience* **105**, 43–53 (2001).
15. Salio, M. *et al.* Cardioprotective function of the long pentraxin PTX3 in acute myocardial infarction. *Circulation* **117**, 1055–1064 (2008).
16. Mold, C., Rodriguez, W., Rodic-Polic, B. & Du Clos, T.W. C-reactive protein mediates protection from lipopolysaccharide through interactions with FcγR. *J. Immunol.* **169**, 7019–7025 (2002).
17. Rodriguez, W. *et al.* C-reactive protein-mediated suppression of nephrotoxic nephritis: role of macrophages, complement, and Fcγ receptors. *J. Immunol.* **178**, 530–538 (2007).
18. Tennent, G.A. *et al.* Transgenic human CRP is not pro-atherogenic, pro-atherothrombotic or pro-inflammatory in apoE–/– mice. *Atherosclerosis* **196**, 248–255 (2008).
19. Noursadeghi, M. *et al.* Role of serum amyloid P component in bacterial infection: protection of the host or protection of the pathogen. *Proc. Natl. Acad. Sci. USA* **97**, 14584–14589 (2000).
20. Vestweber, D. & Blanks, J.E. Mechanisms that regulate the function of the selectins and their ligands. *Physiol. Rev.* **79**, 181–213 (1999).
21. Springer, T.A. Traffic signals for lymphocyte recirculation and leukocyte emigration: the multistep paradigm. *Cell* **76**, 301–314 (1994).
22. McEver, R.P. Selectins: lectins that initiate cell adhesion under flow. *Curr. Opin. Cell Biol.* **14**, 581–586 (2002).
23. Lowe, J.B. Glycan-dependent leukocyte adhesion and recruitment in inflammation. *Curr. Opin. Cell Biol.* **15**, 531–538 (2003).
24. Kansas, G.S. Selectins and their ligands: current concepts and controversies. *Blood* **88**, 3259–3287 (1996).
25. Ley, K. & Reutershan, J. Leucocyte-endothelial interactions in health and disease. *Handb. Exp. Pharmacol.* **176**, 97–133 (2006).
26. Hartwell, D.W. & Wagner, D.D. New discoveries with mice mutant in endothelial and platelet selectins. *Thromb. Haemost.* **82**, 850–857 (1999).
27. Mayadas, T.N., Johnson, R.C., Rayburn, H., Hynes, R.O. & Wagner, D.D. Leukocyte rolling and extravasation are severely compromised in P selectin-deficient mice. *Cell* **74**, 541–554 (1993).
28. Yang, J. *et al.* Targeted gene disruption demonstrates that P-selectin glycoprotein ligand 1 (PSGL-1) is required for P-selectin-mediated but not E-selectin-mediated neutrophil rolling and migration. *J. Exp. Med.* **190**, 1769–1782 (1999).
29. Sprong, T. *et al.* Pentraxin 3 and C-reactive protein in severe meningococcal disease. *Shock* **31**, 28–32 (2009).

30. Stibenz, D. *et al.* Binding of human serum amyloid P component to L-selectin. *Eur. J. Immunol.* **36**, 446–456 (2006).
31. Mehta, P., Cummings, R.D. & McEver, R.P. Affinity and kinetic analysis of P-selectin binding to P-selectin glycoprotein ligand-1. *J. Biol. Chem.* **273**, 32506–32513 (1998).
32. Yang, J., Furie, B.C. & Furie, B. The biology of P-selectin glycoprotein ligand-1: its role as a selectin counterreceptor in leukocyte-endothelial and leukocyte-platelet interaction. *Thromb. Haemost.* **81**, 1–7 (1999).
33. Inforzato, A. *et al.* Structure and function of the long pentraxin PTX3 glycosidic moiety: fine-tuning of the interaction with C1q and complement activation. *Biochemistry* **45**, 11540–11551 (2006).
34. Mauri, T. *et al.* Persisting high levels of plasma pentraxin 3 (PTX3) over the first days from severe sepsis and septic shock onset are associated with mortality. *Intensive Care Med.* (published online, doi:10.1007/s00134-010-1752-5 (30 January 2010)).
35. Muller, B. *et al.* Circulating levels of the long pentraxin PTX3 correlate with severity of infection in critically ill patients. *Crit. Care Med.* **29**, 1404–1407 (2001).
36. Inforzato, A. *et al.* Structural characterization of PTX3 disulfide bond network and its multimeric status in cumulus matrix organization. *J. Biol. Chem.* **283**, 10147–10161 (2008).
37. Vestweber, D. The selectins and their ligands. *Curr. Top. Microbiol. Immunol.* **184**, 65–75 (1993).
38. Dole, V.S., Bergmeier, W., Mitchell, H.A., Eichenberger, S.C. & Wagner, D.D. Activated platelets induce Weibel-Palade-body secretion and leukocyte rolling in vivo: role of P-selectin. *Blood* **106**, 2334–2339 (2005).
39. Miotla, J.M., Ridger, V.C. & Hellewell, P.G. Dominant role of L- and P-selectin in mediating CXC chemokine-induced neutrophil migration in vivo. *Br. J. Pharmacol.* **133**, 550–556 (2001).
40. Pinho, V. *et al.* Tissue- and stimulus-dependent role of phosphatidylinositol 3-kinase isoforms for neutrophil recruitment induced by chemoattractants in vivo. *J. Immunol.* **179**, 7891–7898 (2007).
41. Breviario, F. *et al.* Interleukin-1-inducible genes in endothelial cells. Cloning of a new gene related to C-reactive protein and serum amyloid P component. *J. Biol. Chem.* **267**, 22190–22197 (1992).
42. Lee, G.W., Lee, T.H. & Vilcek, J. TSG-14, a tumor necrosis factor- and IL-1-inducible protein, is a novel member of the pentaxin family of acute phase proteins. *J. Immunol.* **150**, 1804–1812 (1993).
43. Mulligan, M.S. *et al.* Protective effects of oligosaccharides in P-selectin-dependent lung injury. *Nature* **364**, 149–151 (1993).
44. Rubenfeld, G.D. *et al.* Incidence and outcomes of acute lung injury. *N. Engl. J. Med.* **353**, 1685–1693 (2005).
45. Ware, L.B. & Matthay, M.A. The acute respiratory distress syndrome. *N. Engl. J. Med.* **342**, 1334–1349 (2000).
46. Zarbock, A., Singbartl, K. & Ley, K. Complete reversal of acid-induced acute lung injury by blocking of platelet-neutrophil aggregation. *J. Clin. Invest.* **116**, 3211–3219 (2006).
47. Reading, P.C. *et al.* Antiviral activity of the long chain pentraxin PTX3 against influenza viruses. *J. Immunol.* **180**, 3391–3398 (2008).
48. Kaneko, Y., Nimmerjahn, F. & Ravetch, J.V. Anti-inflammatory activity of immunoglobulin G resulting from Fc sialylation. *Science* **313**, 670–673 (2006).

ONLINE METHODS

Proteins. Recombinant human and mouse PTX3 and the PTX3 C-terminal and N-terminal domains were purified under endotoxin-free conditions by immunoaffinity, ion-exchange chromatography and gel filtration, respectively, from the supernatants of stably transfected CHO cells as described[14]. Enzymatically deglycosylated PTX3 was obtained as described[26]. All proteins were at least 95% pure as assessed by SDS-PAGE followed by silver staining. PTX3 was deglycosylated by site-directed mutagenesis (Tecnogen). Recombinant human P-selectin, E-selectin, L-selectin and the PSGL-1–Fc chimera were from R&D Systems. Polyclonal antibody to PTX3 was prepared by immunization of rabbits with purified human recombinant PTX3. Function-blocking monoclonal antibody to mouse P-selectin (Rb40.34)[49] was a gift from D. Vestweber.

Cells. P-selectin-transfected CHO cells were a gift from G. Kansas. Untransfected CHO cells (American Type Culture Collection) and D6-transfected CHO cells (a gift from M. Locati) served as control cells for binding experiments. Venous blood was collected from healthy volunteers (after informed consent was provided) as approved by the Ethical Committee of Istituto Clinico Humanitas. Blood was drawn with an 18-gauge needle and dripped freely into open tubes containing 3.8% (vol/vol) sodium citrate (1:9, sodium citrate/blood). Tubes were centrifuged for 15 min at 100*g*. Platelet-rich plasma was collected and platelets were washed once (10 min at 300*g*) and resuspended in HEPES Tyrode buffer, pH 7.4, containing $CaCl_2$ (2.5 mM). Human neutrophils were purified from the blood of healthy donors by density gradients as described[11].

Animals. *Ptx3*$^{-/-}$ mice were generated as described[3] and were used on a C57BL/6J or 129/Sv inbred genetic background matched with the appropriate wild-type controls (Charles River Laboratories). P-selectin-deficient mice (on a C57BL/6 genetic background) were a gift from V. Evangelista. Procedures involving animals and their care conformed with institutional guidelines in compliance with national laws and policies (Decretto Legge number 116, Gazzetta Ufficiale supplement 40, 18-2-1992) and international laws and policies (European Economic Community Council (1987), Directive 86/609, Official Journal of European Communities, Law 358,1; National Institutes of Health Guide for the Care and Use of Laboratory Animals, US National Research Council 1996). Mice were housed in the specific pathogen–free animal facility of the Istituto Clinico Humanitas in individually ventilated cages and were used between 6 and 12 weeks of age.

Microtiter plate assays. Microtiter plates (Nunc) were coated with P-selectin, E-selectin, L-selectin or C1q (each at a concentration of 5 μg/ml) in PBS^{2+} phosphate buffer (containing $CaCl_2$ (130 mg/l) and $MgCl_2$ (100 mg/l); Lonza) by overnight incubation at 4 °C. Nonspecific binding to the plates was blocked by incubation for 2 h at 25 °C with 5% (wt/vol) dry milk in PBS. All reaction volumes were 100 μl and plates were washed after each step with PBS^{2+} containing 0.05% (vol/vol) Tween-20. Single binding experiments and concentrations of ligands are noted in the figure legends. Binding was detected by incubation with polyclonal rabbit antibody to human PTX3 (1:2,000 dilution; made 'in-house'), followed by horseradish peroxidase–conjugated secondary antibody to the species (Jackson ImmunoResearch). Tetramethylbenzidine substrate (Sigma) was used, and absorbance was measured at 450 nm.

SPR. The ProteOn XPR36 Protein Interaction Array system (Bio-Rad) was used for binding studies. Full-length human PTX3 and its C-terminal domain were covalently immobilized onto two flow cell surfaces of the same Proteon GLC sensor chip (Bio-Rad) by standard amine-coupling protocols. For the immobilization step, the ligands were diluted to a final concentration of 20–30 μg/ml in acetate buffer (pH 2.5 for PTX3; pH 3.7 for the PTX3 C-terminal domain). The amount of PTX3 or the PTX3 C-terminal domain covalently immobilized on the surface, presented as resonance units (1 resonance unit = 1 pg protein/mm^2), was about 2,000–3,000 or 1,000–2,000, respectively. A reference channel was always prepared in parallel by the same activation-deactivation procedure but with the injection of vehicle only. The analyte running buffer was Tris-HCl, pH 7.4, containing 150 mM NaCl, 1.2 mM $CaCl_2$ and 0.005% (vol/vol) Tween 20. P-selectin was injected over immobilized ligands for 2–3 min at a rate of 30 μl/min (association phase), and dissociation was measured in the subsequent 10–15 min. Vehicle (running buffer) was always injected in parallel flow channels. Where needed, complete dissociation of bound analytes was induced by a 30-second injection with 2 M NaCl (regeneration step). ProteOn analysis software was used for analysis of sensorgrams.

Flow cytometry. Purified human platelets (1×10^8 platelets per sample), resting or activated with thrombin (1 U/ml; Sigma), were incubated for 30 min at 25 °C with 1 μM biotinylated PTX3 in the presence or absence of function-blocking monoclonal antibody to human P-selectin (20 μg/ml; CLB-Thromb/6; Immunotech). Samples were then washed with HEPES Tyrode buffer, pH 7.4, and were fixed with PBS containing 1% (vol/vol) formaldehyde. After being stained with allophycocyanin-conjugated streptavidin, samples were analyzed with a FACSCanto (BD) and FACSDiva software (BD). In another set of experiments, the binding of various doses of biotinylated PTX3 to P-selectin-transfected, D6-transfected and untransfected CHO cells (all at a density of 1×10^6 cells per sample) was evaluated. After 1 h of incubation at 4 °C, samples were washed, stained with phycoerythrin-conjugated streptavidin and analyzed with a FACSCanto (BD), FACSDiva software (BD) and FlowJo software.

Leukocyte rolling assay. Microcap glass capillary tubes (100 μl; Drummond) were coated for 10 h at 4 °C with 20 μl human E-selectin or P-selectin (1 μg/ml dissolved in PBS; R&D Systems); some tubes coated previously with E-selectin or P-selectin were also further coated for 16 h with 20 μl PTX3 (various concentrations dissolved in PBS). Immediately before use, tubes were washed extensively and human PMNs, resuspended at a density of 0.5×10^6 cells per ml, a solution of 2 mM Ca^{2+} and Mg^{2+} and 10% (vol/vol) FCS in PBS, were fluxed into the tubes at a shear stress of 2 dyne/cm^2. The activity of interacting cells was recorded on S-VHS videotape and was analyzed frame by frame by computer-assisted digital analysis[50]. Single areas of 0.2 mm^2 were recorded for at least 30 s. Rolling interactions (corresponding to interactions lasting less than 0.5 s) were considered important and were assigned scores.

Bone marrow transplantation. C57BL/6J wild-type or *Ptx3*$^{-/-}$ mice were lethally irradiated with a total dose of 900 cGy. Then, 2 h later, mice were injected in the tail vein with 5×10^6 nucleated bone marrow cells obtained by flushing of the cavity of a freshly dissected femur from a wild-type or *Ptx3*$^{-/-}$ donor. Recipient mice received gentalyn (0.4 mg/ml in drinking water) starting 10 d before irradiation and maintained thereafter. At 8 weeks after bone marrow transplantation, the pleural inflammation model was generated.

Pleural inflammation. Intrapleural injection of KC (CXCL1), a known model of the migration of neutrophils into pleural cavity, has been described[29]. Wild-type or *Ptx3*$^{-/-}$ 129/Sv or C57BL/6J mice were injected intrapleurally with 50 μl sterile PBS or 0.1 μg recombinant mouse KC (R&D Systems) and were killed after 2 h. All cells in the pleural fluid were collected by washing of the cavity with 1 ml RPMI medium. Cells were counted in a Burker chamber with Turk's stain. Differential cell counts were made according to standard morphologic criteria to identify cell types in cytospin preparations (Cytospin 4 Cytocentrifuge; Shandon) stained with the Diff-Quik staining kit (Medion Diagnostics). At least 400 cells were counted in each sample.

Acid-induced acute lung injury. Mice anesthetized by intraperitoneal injection of 2.5% Avertin (400 mg per kg body weight; Tribromoethanol, Sigma-Aldrich) were intubated orotracheally with a 22-gauge angiocatheter and ventilated with tidal volume of 8–10 ml per kg body weight at a respiratory rate of 130 min^{-1} and an FiO_2 (fraction of inspired oxygen) of 0.21 and without positive end-expiratory pressure. A 26-gauge plastic cannula was introduced through a tracheotomy and mice received HCl, pH = 1.5 (2 ml per kg body weight) or 0.9% saline. Mechanical ventilation was stopped 10 min after instillation and mice were extubated and placed in an oxygenated chamber (FiO_2 0.5) for 3 h. After mice were killed, bronchoalveolar lavage fluid was collected (three lavages with 1 ml RPMI medium each). All cells in the bronchoalveolar lavage fluid were counted in a Burker chamber and differential cell counts were

done as described above. After bronchoalveolar lavage fluid was collected, the inferior vena cava was opened and nonadherent PMNs were dislodged from the pulmonary vasculature by the flushing of 5 ml PBS through the right ventricle. Lungs were removed and minced, and samples were incubated for 30 min at 37 °C with collagenase type IV (Sigma). Cells were collected after passage through a cell strainer (BD Biosciences) and lysis of red blood cells. Total lung cells were counted in a Burker chamber and differential cell counts were done as described above.

Intravital microscopy in mesenteric venules. Female C57BL6/J (wild-type) and *Ptx3*$^{-/-}$ mice 6–8 weeks of age were housed and used according to European Community rules for the use of laboratory animals. Mice were anesthetized by intraperitoneal injection of physiological saline (10 ml per kg body weight) containing ketamine (5 mg/ml) and xylazine (1 mg/ml). A heparinized polyethylene catheter (PE50; internal diameter, 0.58 mm; Becton Dickinson) was inserted in the lateral tail venule with a 25-gauge needle. After the abdominal fur was shaved, a midline incision was made through the skin and peritoneum. Mice were placed on one side and a segment of the terminal ileum with its accompanying mesentery was exteriorized through the abdominal incision. All exposed tissue was irrigated with phosphate buffer containing thrombin from bovine plasma (0.5 U/ml; Sigma) and was covered with a glass slide to minimize tissue dehydration. All parts of the intestine that were not observed microscopically were covered with soaked cotton pads. The recipient was maintained at 37 °C with a stage-mounted Linkam CO102 strip heater (Olympus) as described[51]. The preparation was placed on a BX50WI microscope (Olympus). The mesenteric vascular bed was visualized with a 16× objective. After 30 min of stimulation with thrombin, PMNs were slowly injected through the catheter. PMNs were suspended at a density of 30×10^6 cells per ml in DMEM without sodium bicarbonate, supplemented with 20 mM HEPES, pH 7.1 and 5% (vol/vol) FCS and were labeled for 10 min at 37 °C with orange fluorescent tetramethylrhodamine (Molecular Probes). Images were visualized with a silicon-intensified target video camera (VE-1000 SIT; Dage-MTI) and a Sony SSM-125CE monitor. Recordings were digitalized and stored on videotapes with a digital VCR (Panasonic NV-DV10000) and Casablanca digital system (MS MacroSystem Computer). Three to six venules (25–55 mm in diameter) were selected in each experiment and a 250-mm length of each venule was observed throughout the experiment.

Video analysis was made by playback of digital videotapes in real time or at lower speed, and frame by frame. Vessel diameter (D), hemodynamic parameters and the velocity of rolling were determined with Image 1.62 software (National Institutes of Health). The velocity of 20 or more consecutive freely flowing cells per venule was calculated, and from the velocity of the fastest cell in each venule (V_{fast}), the mean blood flow velocity (V_m) was calculated as $V_m = V_{fast} / (2 - \varepsilon^2)$, where ε is the ratio of lymphocyte diameter to vessel diameter. The wall shear rate (WSR) was calculated as $WSR = 8 \times V_m / D$ (s^{-1}), and the shear stress (WSS) acting on rolling cells was approximated by WSR × 0.025 (dyn/cm^2), with the assumption of a blood viscosity of 0.025 Poise. Leukocytes were considered to be rolling if they traveled at a velocity below the critical velocity ($V_{crit} = V_m \times \varepsilon \times (2 - \varepsilon)$)[52]. At least 150 consecutive cells per venule were examined. Rolling fractions were defined as the percentage of cells that rolled within a given venule among the total number of cells that entered that venule during the same period[53].

Statistical analysis. Data were compared by one-way ANOVA followed by the Newman-Keuls multiple comparison test with Prism software (version 4.00 for Windows; GraphPad) or with the paired or unpaired two-tailed Student's *t*-test.

Additional methods. Information on the preparation of PMNs for intravital microscopy and the assessment of pressure-volume curves is available in the **Supplementary Methods**.

49. Kunkel, E.J. *et al.* Absence of trauma-induced leukocyte rolling in mice deficient in both P-selectin and intercellular adhesion molecule 1. *J. Exp. Med.* **183**, 57–65 (1996).
50. Bolomini-Vittori, M. *et al.* Regulation of conformer-specific activation of the integrin LFA-1 by a chemokine-triggered Rho signaling module. *Nat. Immunol.* **10**, 185–194 (2009).
51. Piccio, L. *et al.* Molecular mechanisms involved in lymphocyte recruitment in inflamed brain microvessels: critical roles for P-selectin glycoprotein ligand-1 and heterotrimeric G_i-linked receptors. *J. Immunol.* **168**, 1940–1949 (2002).
52. Ley, K. & Gaehtgens, P. Endothelial, not hemodynamic, differences are responsible for preferential leukocyte rolling in rat mesenteric venules. *Circ. Res.* **69**, 1034–1041 (1991).
53. Fabene, P.F. *et al.* A role for leukocyte-endothelial adhesion mechanisms in epilepsy. *Nat. Med.* **14**, 1377–1383 (2008).

doi:10.1038/ni.1854